Journal of Power Sources 181 (2008) 172–176

Contents lists available at ScienceDirect

Journal of Power Sources

journal homepage: www.elsevier.com/locate/jpowsour

Short communication

High-performance polypyrrole nanoparticles counter electrode for dye-sensitized solar cells

Jihuai Wu*, Qinghua Li, Leqing Fan, Zhang Lan, Pinjiang Li, Jianming Lin, Sanchun Hao

The Key Laboratory of Functional Materials for Fujian Higher Education, Institute of Materials Physical Chemistry, Huaqiao University, Quanzhou 362021, China

ARTICLE INFO

Article history:
Received 28 November 2007
Received in revised form 4 March 2008
Accepted 4 March 2008
Available online 22 March 2008

Keywords:
Dye-sensitized solar cell
Polypyrrole nanoparticle
Counter electrode

ABSTRACT

Polypyrrole (PPy) nanoparticle was synthesized and coated on a conducting FTO glass to construct PPy counter electrode used in dye-sensitized solar cell (DSSC). Scanning electron microscope images show that PPy with porous and particle diameter in 40–60 nm is covered on the FTO glass uniformly and tightly. Cyclic voltammograms of I_2/I^- system measurement reveals that the PPy electrode has smaller charge-transfer resistance and higher electrocatalytic activity for the I_2/I^- redox reaction than that Pt electrode does. Overall energy conversion efficiency of the DSSC with the PPy counter electrode reaches 7.66%, which is higher (11%) than that of the DSSC with Pt counter electrode. The excellent photoelectric properties, simple preparation procedure and inexpensive cost allow the PPy electrode to be a credible alternative used in DSSCs.

1. Introduction

Since the prototype of a dye-sensitized solar cell (DSSC) was reported in 1991 by O'Regan and Gratzel [1], it has aroused intensive interest over the past decade due to its low cost and simple preparation procedure [2–6]. In general, the DSSC has a sandwich structure with two transparent conductive glass substrates. The cell consists of an electrode composed of a porous nanocrystalline TiO_2 film sensitized by a dye for absorbing visible light, a redox electrolyte, and a platinized counter electrode to collect electrons and catalyze I_2/I^- redox-coupled regeneration reaction in electrolyte. The principle of operation of the DSSC involves the photoexcitation of the sensitizer, followed by electron injection into the conduction band of the semiconductor oxide film. The dye molecule is regenerated by the redox system, which itself is regenerated at the counter electrode by electrons passing through the load.

Counter electrode of DSSC is usually made of platinum, which has high conductivity, stability and catalytic activity for I_2 reduction. But platinum is one of the expensive components in DSSC [7]. Recently, to reduce the production cost of DSSC, porous carbon materials are attempted to replace platinum electrode, however, the conversion efficiency of the DSSC based on the carbon electrode is relatively low due to the poor catalytic activity for I_2 reduction and lower conductivity of carbon [8–11].

The conducting polymers are promising candidates as counter electrode materials used in DSSC, because of their unique properties, such as inexpensive, high conductivity, remarkable stabilities, good specific capacitances, and catalytic activity for I_2 reduction [12–15]. However, there are only a few reports on the conducting polymer as a counter electrode material using in DSSC. The polypyrrole (PPy) is one of the most intensively studied conducting polymers during the last decade. Beside its mechanical and chemical stability and high conductivity, polypyrrole is synthesized easily by electrochemical method in aqueous media [16–18]. Up to present, the polypyrrole has been employed to construct PPy/TiO_2 anode or solid electrolyte used in DSSC, and the photoelectric performance of the DSSC was improved [19–21].

In this paper, the PPy nanoparticle was synthesized and coated on a conducting FTO glass to construct PPy counter electrode used in DSSC. It is expected that photoelectric performances of the DSSC with PPy electrode can be improved.

2. Experimental

2.1. Synthesis of polypyrrole nanoparticle

The pyrrole monomer (Merck) used for the present study was purified by a vacuum distillation before using. All solvents were used without further treatment before using. All work was carried out in ambient atmosphere, unless specified otherwise. The PPy nanoparticle was synthesized as follows [22]. One gram of solid iodine was added into 200 mL of alcohol and distilled water solution with a volume ratio of 1:1. And then 1.5 mL of pyrrole (Py) monomer was added dropwise onto the surface of the solution. The beaker was covered with aluminium foil and kept in the dark at 4 °C for at least 48 h. As Py diffused slowly into the aqueous medium,

* Corresponding author. Tel.: +86 595 22693899; fax: +86 595 22693999.
E-mail address: jhwu@hqu.edu.cn (J. Wu).

0378-7753/$ – see front matter © 2008 Published by Elsevier B.V.
doi:10.1016/j.jpowsour.2008.03.029

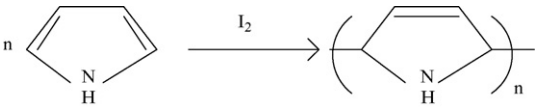

Scheme 1. The synthetic chemical reaction of PPy.

the solution changed gradually from the original pink color of I_2 to dark green color, at the same time some black material was formed. The mixture was filtered and the black material was collected, and the black material was rinsed adequately with enough amounts of methanol, acetonitrile, carbon tetrachloride, and then soaked in a excess of absolute ethanol for at least 48 h. Finally it was subjected to ultrasonic irradiation with a power of 100 W for 10 h. After sonication for 2 h, the black material was filtered and dried at 80 °C to remove residue solvent. The resultant black material was designated PPy nanoparticles. The PPy nanoparticles so produced were spongy and somewhat rubbery in texture. The yield was about 50%. Scheme 1 shows the chemical equation of the reaction.

2.2. Assembling of DSSCs

The FTO glasses (sheet resistance 10 Ω cm^{-2}, Hartford Glass Co., USA) were cleaned and activated in the concentrated system $C_{16}H_{33}N(C_2H_5)_3Br$/DS–10 (volume ratio, 5:95) at 35 °C for 10 s, and then washed several times with ethanol [23].

2 g of PPy was dispersed into the mixed solution (200 mL) of alcohol and distilled water with a volume ratio of 1:1. The pretreated FTO glass was laid on the bottom of the solution. To control PPy deposited on the FTO glass evenly, the system was stirred continuously for 48 h. After it was subjected to ultrasonic irradiation for 2 h, a PPy electrode was prepared. The PPy electrode was then washed several times with acetonitrile and dried in a nitrogen atmosphere before assembling the DSSC.

Nanoporous TiO_2 film was prepared by the following procedure [24,25]. Tetrabutyltitanate (20 mL) was rapidly added to distilled water (200 mL), a white precipitate was formed immediately. The precipitate was filtered using a glass frit and washed three times with 100 mL distilled water. The filter cake was added to nitric acid aqueous solution (0.1 M, 200 mL) under vigorous stirring at 80 °C until the slurry became a translucent blue-white liquid. The resultant colloidal suspension was autoclaved at 200 °C for 12 h to form a white milky slurry. The resultant slurry was concentrated to one-fourth of its original volume, then PEG-20000 (10 wt.% slurry) and a few drops of emulsification reagent of Triton X-100 were added to form a TiO_2 colloid.

The FTO glass plate was immersed in an isopropanol solution for 48 h to remove any impurities. Then it was cleaned in Triton X-100 aqueous solution, washed with ethanol, and treated with 50 mM $TiCl_4$ aqueous solution at 70 °C for 30 min to make a good interfacial contact between the TiO_2 layer and the conducting glass plate. A plastic adhesive tape was fixed on the four sides of the conducting glass sheet to restrict the thickness and area of TiO_2 porous film. The TiO_2 colloid was dropped on the FTO glass plate by using a doctor scraping technique. The process was done for three times to form a thick TiO_2 film. The TiO_2 film was treated with 50 mM $TiCl_4$ aqueous solution again and washed with distilled water before sintering at 450 °C in air for 30 min. Finally, the TiO_2 porous film was sintered by firing the conducting glass sheet at 450 °C in air for 30 min. After cooling to 80 °C, the TiO_2 film was immersed in an 2.5×10^{-4} M absolute ethanol solution of *cis*-$[(dcbH_2)_2Ru(SCN)_2]$ for 24 h to absorb the dye adequately, then the dye-sensitized TiO_2 film was washed with anhydrous ethanol and dried in moisture-free air.

Dye-sensitized solar cell was assembled [26–28] by injecting an electrolyte into the aperture between the TiO_2 porous film electrode (anode electrode) and the PPy electrode (counter electrode). The two electrodes were clipped together and a cyanoacrylate adhesive was used as sealant to prevent the electrolyte solution from leaking. Epoxy resin was used for further sealing the cell.

2.3. Measurement and characterization

Micromorphology of polypyrrole nanoparticles and polypyrrole electrode were observed by using JSM-6700F field emission scanning electron microscope (FESEM). Fourier transform infrared spectra (FTIR) of samples were recorded on a Nicolet Nexus 470 spectrometer using KBr pellets. Energy dispersive X-ray (EDX) of sample was measured by an INCA-2000 spectrum. Cyclic voltammetry (CV) of samples were measured in a three-electrode one-compartment cell with a polypyrrole nanoparticle coated on FTO working electrode, Pt foil counter electrode and an Ag/AgCl reference electrode dipped in an acetonitrile solution of 10 mM LiI, 1 mM I_2, and 0.1 M $LiClO_4$. CV was performed using CHI660B electrochemical measurement system (scan condition: 20–200 mV s^{-1}).

The photovoltaic test of DSSC was carried out by measuring the *J–V* character curves under simulated AM 1.5 solar illumination at 100 mW cm^{-2} from a 100-W xenon arc lamp (XQ-500W, Shanghai Photoelectricity Device Company, China) in ambient atmosphere; the fill factor (FF) and overall light-to-electrical energy conversion efficiency (η) of DSSC were calculated according to the following

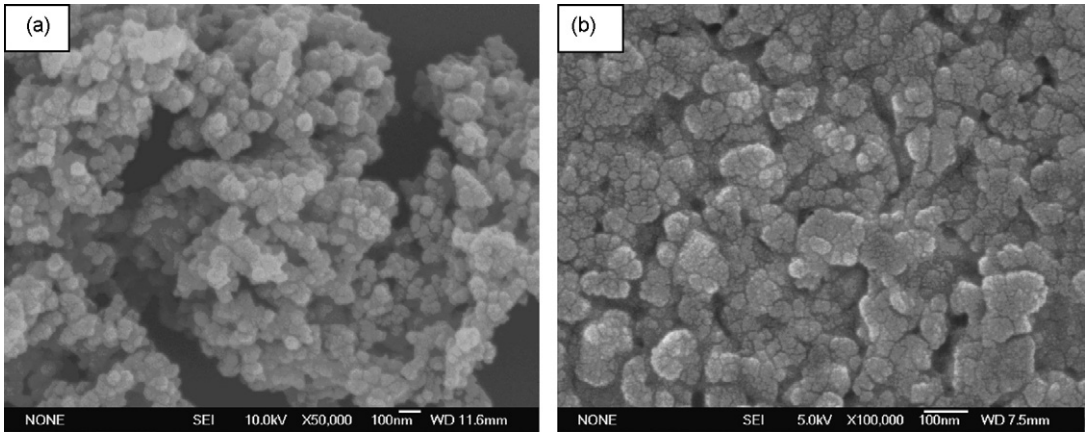

Fig. 1. SEM image of polypyrrole nanoparticles (a) and polypyrrole coated on FTO glass (b).

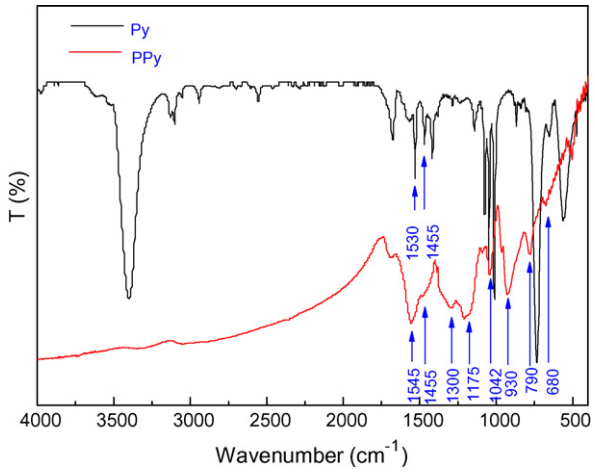

Fig. 2. FTIR spectra of PPy nanoparticles and Py monomer.

equations [29]:

$$FF = \frac{V_{max} J_{max}}{V_{OC} J_{SC}} \quad (1)$$

$$\eta(\%) = \frac{V_{max} J_{max}}{P_{in}} \times 100 = \frac{V_{OC} J_{SC} FF}{P_{in}} \times 100 \quad (2)$$

where J_{SC} is the short-circuit current density (mA cm^{-2}), V_{OC} is the open-circuit voltage (V), P_{in} is the incident light power, and J_{max} (mA cm^{-2}) and V_{max} (V) are the current density and voltage at the point of maximum power output on the J–V curves, respectively.

3. Results and discussion

3.1. Morphology and compositions of polypyrrole

Fig. 1(a) shows the SEM image of polypyrrole nanoparticles prepared by 10 h ultrasonic irradiation in alcohol solution. It is clear that polypyrrole nanoparticles have been completely separated with a particle diameter of 40–60 nm. Fig. 1(b) shows the SEM image of PPy particles covered on the FTO glass with a magnification of 100,000 times. It can be seen clearly that PPy particles present in an diameter range of 40–60 nm on the FTO glass, and the surface exhibits porous state obviously, which benefits for the improvement of electrocatalytic activity for I_2/I^- redox reaction. However, there is some conglomeration of PPy particles on the surface.

The FTIR spectra of Py monomer and PPy powder are given in Fig. 2, which exhibits all characteristic vibrations of PPy [30,31]. The bands at 1545, 1455 and 1175 cm^{-1} come from pyrrole ring and C–N stretching in PPy, respectively. Because the amount of C=C bonds decreases, the peak at 1455 cm^{-1} become weaker in PPy than that in pyrrole in Fig. 2. The band of 1300 cm^{-1} is ascribed to the deforming vibration of C–H and N–H. The bands at 1042 and 790 cm^{-1} are due to C–C stretching vibration, C–H deforming and C–H wagging vibrations, respectively. The low absorption band at 680 cm^{-1} is due to C–H out of plane bending of pyrrole moiety in PPy.

The energy dispersive X-ray analysis of the PPy electrode is shown in Fig. 3, which confirms the presence of nitrogen, iodine, and carbon, the results are consistent with the compositions of PPy.

3.2. Electrochemical properties of PPy counter electrode

Cyclic voltammetry was carried out in an N_2-purged acetonitrile solution. A Pt electrode or a PPy electrode was used as working electrode. A Pt coil as the counter electrode, and an Ag/Ag$^+$ electrode as reference electrode. The electrolyte was the acetonitrile solution

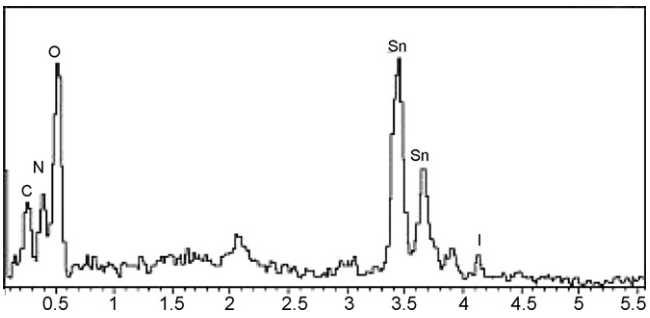

Fig. 3. EDS analysis of the PPy electrode.

containing 0.1 M $LiClO_4$ as the supporting electrolyte and 10 mM LiI, 1 mM I_2 as the redox couple.

Fig. 4 compares cyclic voltammograms of I_2/I^- system for PPy electrode and Pt electrode at a scan rate of 50 mV s^{-1} and $[I^-]/[I_2] = 10/1$. More negative pair is assigned to redox reaction (3) and more positive one is assigned to redox reaction (4) [32]:

$$I_3^- + 2e^- = 3I^- \quad (3)$$

$$3I_2 + 2e^- = 2I_3^- \quad (4)$$

In DSSC, electrons are injected to photooxidized dye from I^- ions in electrolyte (Eq. (4)), and the produced I_3^- are reduced on the counter electrode (Eq. (3)). Fig. 4 shows a much higher current density of the I_3^- reduction peak for the PPy electrode than that for the Pt electrode. This suggests a faster reaction rate on the PPy electrode than that on the Pt electrode. In other words, the charge-transfer resistance (R_{CT}) for the I_2/I^- redox reaction is smaller on the PPy electrode compared with the Pt electrode under the same conditions [33]. And it can be observed clearly that the formal potential shifted more positive for the PPy electrode than the Pt electrode in Fig. 4. Thus, the polypyrrole nanoparticle has a higher electrocatalytic activity in I_2/I^- redox reaction than that of Pt particle.

Fig. 5(a) shows consecutive cyclic voltammograms of I_2/I^- system for PPy electrode from +0.35 to −0.85 V (versus Ag/AgCl) in the acetonitrile solution containing 0.1 M $LiClO_4$ as the supporting electrolyte and 10 mM LiI, 1 mM I_2 as the redox couple, and Pt foil is used as working electrode and the scan rate is 20 mV s^{-1}. Two redox couples are observed. On successive scans, the peak currents density change with the change of scan rate. It indicates that

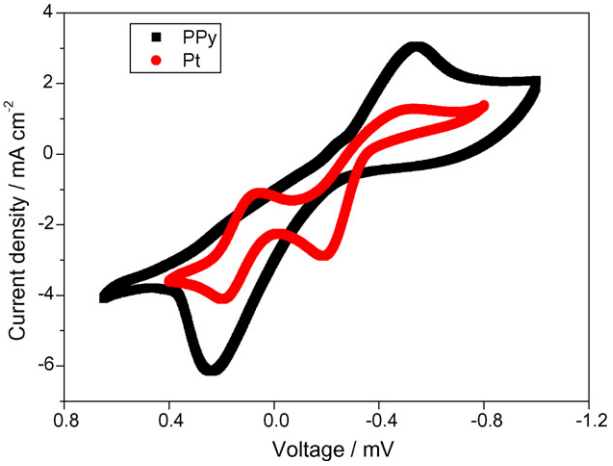

Fig. 4. Cyclic voltammograms for PPy electrode and Pt electrode at a scan rate of 50 mV s^{-1} in 10 mM LiI, 1 mM I_2 acetonitrile solution containing 0.1 M $LiClO_4$ as the supporting electrolyte.

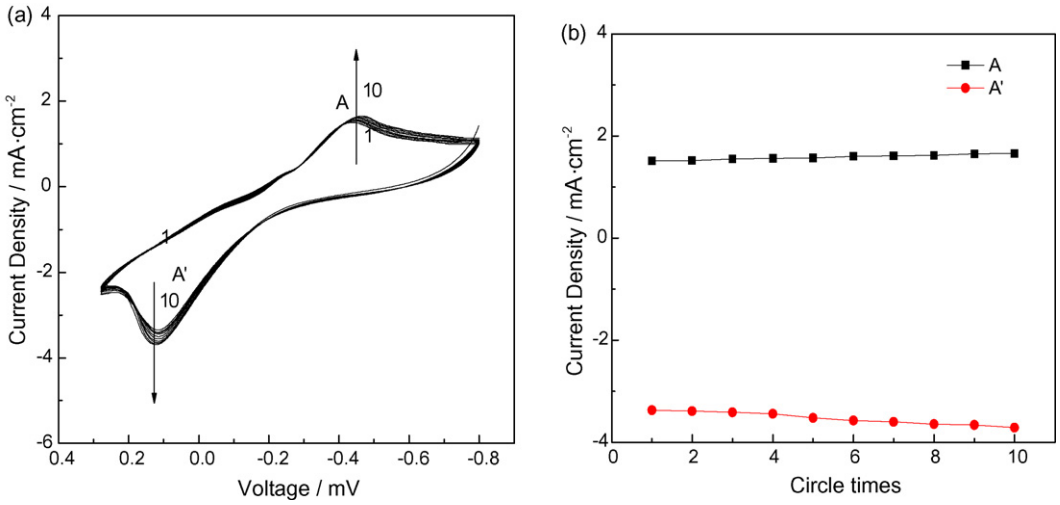

Fig. 5. (a) Consecutive 10 cyclic voltammograms of I_2/I^- system for PPy electrode in the acetonitrile solution containing 0.1 M $LiClO_4$ as the supporting electrolyte and 10 mM LiI, 1 mM I_2 as the redox couple, and Pt foil as working electrode and $\upsilon = 20\,mV\,s^{-1}$. (b) The relationship between the cycle times and the two redox peak currents for PPy electrode.

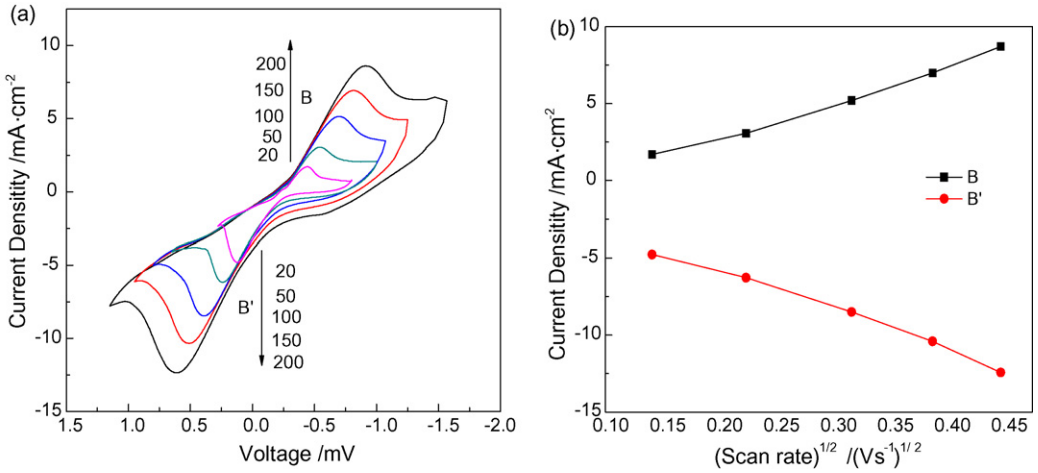

Fig. 6. (a) Cyclic voltammograms for the PPy electrode in acetonitrile solution of 0.1 M $LiClO_4$, 10 mM LiI, 1 mM I_2 with different scan rates (from inner to outer: 20, 50, 100, 150, and 200 mV s^{-1}, respectively). (b) Relationship between all the redox peak currents and scan rates.

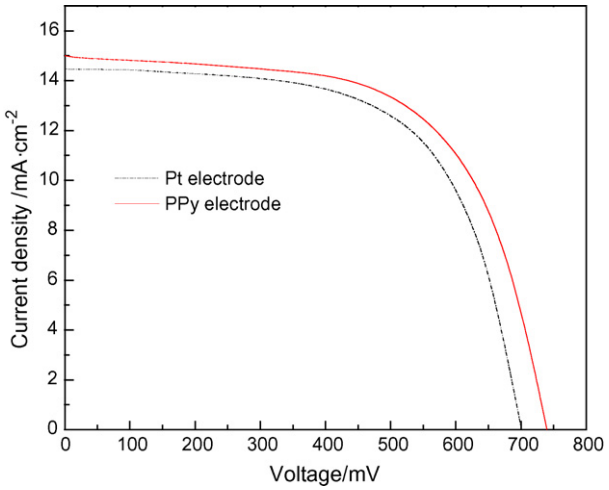

Fig. 7. Photocurrent–voltage characteristics of DSSCs with PPy (solid line) and Pt (dash line) counter electrodes under 100 mA cm^{-2} light irradiation.

the polypyrrole nanoparticles are coated tightly on the FTO glass surface. Both redox peak currents show good linear relationship with the cycle times, as shown in Fig. 5(b). Therefore, it also indicates that the PPy film is uniform and homogeneous [34].

Fig. 6(a) shows cyclic voltammograms of the I_2/I^- system on the PPy electrode with different scan rates in acetonitrile solution of 0.1 M $LiClO_4$, 10 mM LiI, and 1 mM I_2. It can be found that the absolute values of cathodic peak currents are almost the same as that of the corresponding anodic peak currents. The cathodic peak gradually and regularly shifts to the negative direction and the corresponding anodic peak shifts to the positive direction with increasing scan rate. Fig. 6(b) illustrates a relationship between the cathodic and anodic peak currents and the square root of the

Table 1
Photoelectric properties of DSSCs with PPy and Pt counter electrodes

Electrode	J_{SC} (mA cm^{-2})	V_{OC} (mV)	FF	η (%)
PPy	15.01	740	0.69	7.66
Pt	14.47	701	0.68	6.90

Condition: liquid electrolyte contains 0.1 M KI, 0.01 M I_2, and 0.6 M tetrabutylammonium iodide and acetonitrile.

scan rate. The good linear relationship with various scan rates indicates the diffusion limitation of the redox reaction on PPy electrode, which may be connected with transport of iodide species out of the PPy electrode surface [12,35]. This phenomenon shows that the adsorption of iodide species affected the redox reaction on the PPy electrode surface, and this also suggests that no specific interaction between I_2/I^- redox couple and PPy electrode as in the case of Pt electrode and *p*-toluenesulfonate doped poly(3,4-ethylene dioxythiophene) electrode under similar conditions [12,36].

3.3. Photoelectric performance of DSSC with PPy electrode

The photocurrent–voltage curves (Fig. 7) of the DSSCs with PPy counter electrode and Pt counter electrode were measured under irradiation of 100 mW cm^{-2}. And the photoelectric parameters of DSSCs such as short-circuit photocurrent density (J_{sc}), open circuit voltage (V_{oc}), fill factor (FF) and the overall energy conversion efficiency (η) are listed in Table 1. Comparing DSSC with Pt electrode, all photoelectric parameters of the DSSC with PPy electrode are increased. The overall energy conversion efficiency of DSSC with PPy electrode reaches 7.66%, which is improved 11.01% compared with the DSSC with Pt electrode.

The improvement of photoelectric performances of DSSC with PPy counter electrode mainly comes from three aspects. Firstly, the counter electrode covered with porous PPy nanoparticles engenders a large surface area on the electrode. The photoelectric performance of DSSCs can be improved with the increase of surface area of the electrode [9,10,12], especially, it can benefit for the increase of rate of I_2/I^- redox reaction on the PPy electrode. Secondly, the small charge-transfer resistance R_{CT} at the interface between electrolyte and the electrode for the I_2/I^- redox reaction makes for electrons transferring and photocurrent density enhancing. Thirdly, the higher electrocatalytic activity in I_2/I^- redox reaction of polypyrrole nanoparticle results in the increasing of open circuit voltage. Therefore, the DSSC with PPy counter electrode has predominant photoelectric performance.

4. Conclusions

In summary, PPy nanoparticle was synthesized and coated on a conducting FTO glass to construct PPy counter electrode used in dye-sensitized solar cell. Scanning electron microscope images show that PPy with porous and particle diameter in 40–60 nm is covered on the FTO glass uniformly and tightly. Cyclic voltammograms of I_2/I^- system measurement reveals that the PPy electrode has smaller charge-transfer resistance and higher electrocatalytic activity for the I_2/I^- redox reaction than that Pt electrode does. Overall energy conversion efficiency of the DSSC with PPy counter electrode reaches 7.66%, which is higher (11%) than that of the DSSC with Pt counter electrode under the same conditions. The improvement of photoelectric performances of DSSC with PPy counter electrode mainly comes from larger surface area, small charge-transfer resistance and higher electrocatalytic activity for PPy electrode. The excellent photoelectric properties, simple preparation procedure and inexpensive cost allow PPy electrode to be a credible alternative used in DSSCs.

Acknowledgements

The authors thank for the joint support by the National Natural Science Foundation of China (No. 50572030, 50372022), the Nano-Functional Materials Special Program of Fujian Province (No. 2005HZ01-4), the Key Project of Chinese Ministry of Education (No. 206074) and Specialized Research Fund for the Doctoral Program of Chinese Higher Education (No. 20060385001).

References

[1] B. O'Regan, M. Gratzel, Nature 353 (1991) 737.
[2] U. Bach, D. Lupo, P. Comte, J.E. Moser, F. Weissortel, J. Salbeck, M. Gratzel, Nature 395 (1998) 583.
[3] M. Gratzel, Nature 414 (2001) 338.
[4] J. Wu, Z. Lan, J.M. Lin, M.L. Huang, S.C. Hao, T. Sato, S. Yin, Adv. Mater. 19 (2007) 4006.
[5] J. Wu, S. Hao, Z. Lan, J. Lin, M. Huang, Y. Huang, T. Sato, S. Yin, Adv. Funct. Mater. 17 (2007) 2645.
[6] M. Gratzel, Inorg. Chem. 44 (2005) 6841.
[7] G. Smestad, C. Bignozzi, R. Argazzi, Sol. Energy Mater. Sol. Cells 32 (1994) 259.
[8] A. Kay, M. Gratzel, Sol. Energy Mater. Sol. Cells 44 (1996) 99.
[9] N. Papageorgiou, W.F. Moser, M. Gratzel, J. Electrochem. Soc. 144 (1997) 876.
[10] N. Papageorgiou, P. Liska, A. Kay, M. Gratzel, J. Electrochem. Soc. 146 (1999) 898.
[11] K. Suzuki, M. Yamaguchi, M. Kumagai, S. Yanagida, Chem. Lett. 32 (2003) 28.
[12] Y. Saito, W. Kubo, T. Kitamura, Y. Wada, S. Yanagida, J. Photochem. Photobiol. A 164 (2004) 153.
[13] Y. Saito, T. Kitamura, Y. Wada, S. Yanagida, Chem. Lett. (2002) 1060.
[14] T. Yohannes, O. Inganas, Synth. Met. 107 (1999) 97.
[15] T.C. Wei, C.C. Wan, Y.Y. Wang, Appl. Phys. Lett. 88 (2006) 103122.
[16] A.G. MacDiarmid, Synth. Met. 84 (1997) 27.
[17] E. Kupila, J. Kankare, Synth. Met. 74 (1995) 241.
[18] S. Bereznev, J. Kois, I. Golovtsov, A. Opik, E. Mellikov, Thin Solid Films 511/512 (2006) 425.
[19] G.K.R. Senadeera, T. Kitamura, Y. Wada, S. Yanagida, J. Photochem. Photobiol. A 184 (2006) 234.
[20] H. Nagai, H. Segawa, Chem. Commun. (2004) 974.
[21] T. Kitamura, M. Maitani, M. Matsuda, Y. Wada, S. Yanagida, Chem. Lett. (2001) 1054.
[22] E.T. Kang, T.C. Tan, K.G. Neoh, Y.K. Ong, Polymer 27 (1986) 1958.
[23] R. Skokina, L. Voronchikhina, Russ. J. Appl. Chem. 2002 (1990).
[24] J. Wu, Z. Lan, J. Lin, M. Huang, S. Hao, T. Sato, S. Yin, Adv. Mater. 19 (2007) 4006.
[25] J. Wu, Z. Lan, D. Wang, S. Hao, J. Lin, Y. Huang, S. Yin, T. Sato, Electrochim. Acta 51 (2006) 4243.
[26] J. Wu, Z. Lan, J. Lin, M. Huang, S. Hao, L. Fang, Electrochim. Acta 52 (2007) 7128.
[27] J. Wu, P. Li, S. Hao, H. Yang, Electrochim Acta 52 (2007) 5334.
[28] Z. Lan, J. Wu, J. Lin, M. Huang, J. Power Sources 164 (2007) 921.
[29] M. Gratzel, Prog. Photovoltaics 8 (2000) 171.
[30] R. Singh, J. Kumar, A. Kaur, K.L. Yadav, R. Bhattacharyya, E. Hussain, S. Ali, Polymer 47 (2006) 6042.
[31] M. Liu, Y. Zhang, M. Wang, C. Deng, Q. Xie, S. Yao, Polymer 47 (2006) 3372.
[32] A.I. Popov, D.H. Geske, Am. Chem. Soc. 80 (1958) 1340.
[33] K. Imoto, K. Takahashi, T. Yamaguchi, T. Komura, K. Murata, Sol. Energy Mater. Sol. Cells 79 (2003) 459.
[34] H. Guo, Y. Li, L. Fan, X. Wu, M. Guo, Electrochim. Acta 51 (2006) 6230.
[35] S. Biallozor, A. Kupniewska, Electrochem. Commun. 2 (2000) 480.
[36] A. Hauch, A. Georg, Electrochim. Acta 46 (2001) 3457.